Hindawi Publishing Corporation
Oxidative Medicine and Cellular Longevity
Volume 2012, Article ID 498914, 14 pages
doi:10.1155/2012/498914

Research Article

Detailed Analysis of Apoptosis and Delayed Luminescence of Human Leukemia Jurkat T Cells after Proton Irradiation and Treatments with Oxidant Agents and Flavonoids

Irina Baran,[1] Constanta Ganea,[1] Simona Privitera,[2,3] Agata Scordino,[2,3] Vincenza Barresi,[4] Francesco Musumeci,[2,3] Maria Magdalena Mocanu,[1] Daniele F. Condorelli,[4] Ioan Ursu,[5] Rosaria Grasso,[2,3] Marisa Gulino,[6] Alexandru Garaiman,[1] Nicolò Musso,[4] Giuseppe A. Pablo Cirrone,[2] and Giacomo Cuttone[2]

[1] *Department of Biophysics, "Carol Davila" University of Medicine and Pharmacy, 8 Eroii Sanitari, 050474 Bucharest, Romania*
[2] *Istituto Nazionale di Fisica Nucleare, Laboratori Nazionali del Sud, via S. Sofia, 95125 Catania, Italy*
[3] *Dipartimento di Fisica e Astronomia, Università di Catania, Viale A. Doria 6, 95125 Catania, Italy*
[4] *Sezione di Biochimica e Biologia Molecolare, Dipartimento di Scienze Chimiche, Università di Catania, 6 A. Doria, 95125 Catania, Italy*
[5] *"Horia Hulubei" National Institute for Physics and Nuclear Engineering (IFIN-HH), 30 Reactorului, 077125 Bucharest, Romania*
[6] *Università degli Studi di Enna "Kore", Facoltà di Ingegneria, Architettura e delle Scienze Motorie, Cittadella Universitaria, 94100 Enna, Italy*

Correspondence should be addressed to Irina Baran, baran@ifin.nipne.ro

Received 9 March 2012; Accepted 14 May 2012

Academic Editor: Cristina Angeloni

Following previous work, we investigated in more detail the relationship between apoptosis and delayed luminescence (DL) in human leukemia Jurkat T cells under a wide variety of treatments. We used menadione and hydrogen peroxide to induce oxidative stress and two flavonoids, quercetin, and epigallocatechin gallate, applied alone or in combination with menadione or H_2O_2. 62 MeV proton beams were used to irradiate cells under a uniform dose of 2 or 10 Gy, respectively. We assessed apoptosis, cell cycle distributions, and DL. Menadione, H_2O_2 and quercetin were potent inducers of apoptosis and DL inhibitors. Quercetin decreased clonogenic survival and the NAD(P)H level in a dose-dependent manner. Proton irradiation with 2 Gy but not 10 Gy increased the apoptotic rate. However, both doses induced a substantial G_2/M arrest. Quercetin reduced apoptosis and prolonged the G_2/M arrest induced by radiation. DL spectroscopy indicated that proton irradiation disrupted the electron flow within Complex I of the mitochondrial respiratory chain, thus explaining the massive necrosis induced by 10 Gy of protons and also suggested an equivalent action of menadione and quercetin at the level of the Fe/S center N2, which may be mediated by their binding to a common site within Complex I, probably the rotenone-binding site.

1. Introduction

During the past decades there has been a steadily growing interest in the benefits of natural flavonoids. These compounds which are ubiquitously occurring in fruits, vegetables, and tea possess chemopreventive, cardioprotective, anticancer, anti-inflammatory, antiallergenic, and anti-microbial properties. Epigallocatechine-3-gallate (EGCG) and quercetin (QC; 3,5,7,3′,4′-pentahydroxyflavone) are two well-investigated flavonoids which inhibit cell proliferation and induce apoptosis in various cancer cell types [1–9]. Both EGCG and QC can exert a dual, pro- and antioxidant effect, depending on dosage and time of treatment, and numerous studies have indicated that malignant cells are more susceptible than normal cells to the cytotoxicity of these two flavonoids [2, 7–9]. At present, only a few agents are known to possess such potential for selective/preferential elimination of cancer cells while exerting cytoprotective effects on normal cells [2]. Therefore, this property could be exploited to prevent leukemia or to increase the efficiency of leukemia chemotherapies.

At the moment, the antiproliferative effects of EGCG and QC and their dose dependence in human acute lymphoblastoid leukemia Jurkat T cells are largely unknown. It has been shown that QC can accumulate in large quantities inside the mitochondria, where it is stored in a biologically active form bound to mitochondrial proteins [10]. QC can also act as an activator or inhibitor of the mitochondrial permeability transition pore, depending on its pro- or antioxidant character, respectively [11]. QC is able to inhibit Complexes I and III of the mitochondrial electron transport chain (ETC) [12] and participate in quinone redox cycling [8, 13]. At high doses, QC enhances the cellular production of hydrogen peroxide (H_2O_2) and superoxide ($O_2^{-\bullet}$) [9, 11, 14]. $O_2^{-\bullet}$ can be then dismutated to H_2O_2 by cytosolic or mitochondrial superoxide dismutases. Furthermore, additional $OH^\bullet$ can be produced from H_2O_2 through Fe/Cu-dependent Fenton reactions. At low doses ($\sim 10\,\mu$M) QC exercises protective effects against H_2O_2 but not MD in Jurkat cells [15]. When applied for short periods, quercetin can decrease the cellular H_2O_2 content, whereas in long-term administration it depresses the level of the endogenous antioxidant GSH (reduced glutathione). This in turn may lead to accelerated production of reactive oxygen species (ROS) and toxic metabolites of quercetin [9, 11, 14, 16, 17]. Recent studies have shown that in Jurkat cells low EGCG concentrations ($\sim 10\,\mu$M) exhibit a protective, antioxidant effect, whereas high concentrations ($\sim 100\,\mu$M) have a prooxidant, cyto, and genotoxic effect, inducing DNA lesions even in the absence of exogenous oxidant agents [1]. In Jurkat cells, EGCG ($50\,\mu$M) produces intracellular H_2O_2, which induces apoptosis by a Fe^{2+}-dependent mechanism, through generation of hydroxyl radicals via Fenton reactions [5]. In a different cell type, EGCG has been shown to associate with mitochondria and other yet unidentified cytoplasmic organelles [18].

A clinically important chemotherapeutic agent used in the treatment of leukemia is menadione (vitamin K_3) [6, 19]. Early studies have revealed that menadione (MD) reduction at Complex I of the mitochondrial ETC [20, 21] accounts for ~50% of MD metabolism [21]. As a consequence, MD can increase superoxide production by disrupting the electron flow within Complex I [21]. MD, H_2O_2, EGCG, and QC can activate the apoptotic program in various cell types via a Ca^{2+}-dependent mitochondrial pathway, which is mediated by elevation of cytosolic Ca^{2+} levels and dissipation of the mitochondrial membrane potential [7, 11, 12, 19, 22–26]. However, the current available data on the effects of these compounds on the cell cycle or apoptosis/necrosis in Jurkat cells are extremely limited.

In this work we have extended our previous studies [15] and carried out a thorough investigation of the relationship between apoptosis and delayed luminescence (DL) under a vast range of conditions induced by oxidative stress, flavonoid treatments, and irradiation with 62 MeV proton beams (some preliminary data were reported in [27]). We have performed a detailed analysis of the kinetics of apoptosis induction and cell cycle progression following various treatments. Moreover, we have investigated for the first time the effects of high-energy protons on these cells and found that this type of radiation preferentially induces necrosis, not apoptosis in Jurkat cells, as well as arrest of the cell cycle in the G_2/M phase. This may have relevant implications in radiotherapy, as it is generally known that the radiosensitivity of human leukemia Jurkat T cells is relatively high [25, 28–30]. In addition, it has been reported that high doses (≥ 10 Gy) of X or γ radiation induce significant apoptosis in Jurkat cells, in a time- and dose-dependent manner [25, 29, 30]. Thus, our investigations suggest a differential effect on cell death induction depending on the type of radiation. Moreover, quercetin was able to reduce apoptosis and prolong the G_2/M arrest induced by proton irradiation.

In addition, our current data obtained by DL spectroscopy provide novel insights into the effects of MD, H_2O_2, EGCG, QC, and high-energy protons at the level of mitochondrial Complex I. Delayed luminescence, which is also called "delayed fluorescence", represents a very weak light emission following exposure to pulsed light or UV radiation [31–43]. Its main characteristics are the multicomponent decay pattern of photoemission and the long-time scale of the process. In this work, DL spectroscopy indicated that proton irradiation disrupted the electron flow within Complex I of the mitochondrial respiratory chain and also suggested an equivalent action of menadione and quercetin at the level of Complex I.

2. Materials and Methods

The experiments and methodologies described in this study were generally conducted as described earlier [15, 27, 44].

2.1. Cell Cultures. Human leukemia Jurkat T-cell lymphoblasts were cultured in suspension in MegaCell RPMI 1640 medium supplemented with 5% heat-inactivated fetal bovine serum, 2 mM L-glutamine, 100 units/mL penicillin, and $100\,\mu$g/mL streptomycin, at 37°C in a humidified incubator with a 5% CO_2 atmosphere. Exponentially growing cells were adjusted to a density of 0.2×10^6 cells/mL the day before the experiment. We used hydrogen peroxide 30% solution and stock solutions of menadione sodium bisulphite dissolved in phosphate buffer saline (PBS) or dehydrated quercetin and epigallocatechin gallate dissolved in dimethyl sulfoxide (DMSO). In combined treatments, the oxidant agent was added directly to the cell cultures after preincubation with QC or EGCG as specified, without intermediary wash out. Unless specified otherwise, all chemicals were from Sigma-Aldrich. After each treatment, cells were washed thoroughly with PBS and resuspended in PBS (for DL samples, $\sim 40 \times 10^6$ cells/mL) or in complete medium for apoptosis assessment ($\sim 0.2 \times 10^6$ cells/mL). DL samples were analyzed immediately by DL spectroscopy. Cell density, viability, and morphology were examined with a CCD camera Logitech QuickCam Pro 4000, connected to an Olympus CK30 phase contrast microscope. For cell density assessment, $25\,\mu$L aliquots of the DL samples was diluted in PBS, stained with 0.4% trypan blue solution and ~1500–2000 cells were imaged on a Bürker haemocytometer at the time of the DL assay. Cell count evaluation was performed both during DL experiments, directly by visual inspection under the

microscope, and later on, by analyzing the micrographs with the use of the software ImageJ.

2.2. Proton Irradiation. Cell suspensions (7 mL) were irradiated in 50 mL centrifuge tubes fixed in a vertical position. 62 MeV proton beams accelerated by the superconducting cyclotron at LNS-INFN, Catania (Italy) were used for proton irradiation at a dose rate of 11.76 Gy/min. The proton beams were modulated in the wide-spread Bragg peak configuration, to produce a uniform distribution of the absorbed dose in the entire cell suspension. A plane-parallel advanced PTW 34045 Markus ionization chamber was adopted as a reference dosimeter. The dose measurements were performed in a water phantom, according to International Atomic Energy Agency (IAEA) TRS 398. The absorbed dose to water per monitor unit (cGy/M.U.) was measured at the isocenter, at the depth corresponding to the middle of the modulated beam, with the reference circular collimator (diameter = 25 mm).

2.3. Clonogenic Survival Assay. After the treatment, cells were washed thoroughly with warm PBS and plated in 96 well plates at a plating density of 3, 4, or 10 cells/well in 100 μL of complete medium per well. After 4 weeks of incubation, the plates were inspected by microscopy and the wells containing colonies with >50 cells were counted. The plating efficiency was calculated as $\ln[96/(\text{no. of negative wells})]/(\text{plating density}) \times 100$. Clonogenic survival was calculated as the ratio between the plating efficiency of treated and control cells, respectively.

2.4. Flow Cytometry. At specified times after the treatment, samples containing 10^6 cells were fixed in 70% ethanol and frozen at -20°C. For flow-cytometer determinations, the ethanol-fixed samples were washed with PBS, incubated with a propidium iodide PI/RNAse staining buffer (PHARMINGEN 550825) for 15 min, in the dark at room temperature and analyzed with a Becton Dickinson FACS Calibur flow cytometer. For data acquisition and analysis we used the software CellQuest, WinMDI 2.9 and Cylchred, together with a Gaussian deconvolution algorithm as described [15]. Apoptosis was evaluated as the fraction of hypodiploid cell fragments (the sub-G_0/G_1 cell fraction). The G_0/G_1, S, and G_2/M cell fractions were calculated for the nonapoptotic cell population, by excluding the hypodiploid events from the cell cycle analysis.

2.5. Delayed Luminescence Spectroscopy. We used an improved version of the ARETUSA set-up [39], a highly sensitive equipment able to detect single photons. The cell samples were excited by a Nitrogen Laser source (Laser Photonics LN 230C; wavelength 337 nm, pulse-width 5 ns, energy 100 ± 5 μJ/pulse). A multialkali photomultiplier tube (Hamamatsu R-7602-1/Q) was used as a detector for photoemission signals with wavelengths in the visible range (VIS, 400–800 nm), in single photon counting mode. In some determinations, two broad band (about 80 nm FWHM) Lot-Oriel interferential filters, disposed in a wheel between the sample and the photomultiplier, were used to select photons with wavelength of 460 nm and 645 nm, respectively. The detected signals were acquired by a Multichannel Scaler (Ortec MCS PCI) with a minimum dwell time of 200 ns. DL measurements were done on at least 3 different drops from each cell sample (drop volume 15–25 μL) at room temperature (20 ± 1°C). PBS luminescence was subtracted from all recordings. Photoemission was recorded between 11 μs and 100 ms after laser excitation. DL intensity (I) was obtained as the number of photons recorded within a certain time interval divided to that time interval and to the number of living cells in the drop. The quantum yield was calculated in three time domains of the DL emission: 11–100 μs (DL-I), 100 μs–1 ms (DL-II), and 1–10 ms (DL-III), as the ratio between the I-integral and the energy of the laser. This analysis could not be performed in consistent manner in the time domain 10–100 ms, as in some cases the signal-to-noise ratio was too high within this region.

2.6. Spectrofluorimetry. For determination of the relative level of intracellular nicotinamide adenine dinucleotide and nicotinamide adenine dinucleotide phosphate in their reduced form (NADH and NADPH, resp.), denoted generically as NAD(P)H, exponentially growing cells were washed twice in a standard saline solution (SS) containing 140 mM NaCl, 5 mM KCl, 1 mM $CaCl_2$, 1 mM $MgCl_2$, 20 mM HEPES, and 10 mM glucose, pH 7.2/NaOH, resuspended in SS at $\sim 10^6$ cells/mL, and transferred into a 2 mL quartz cuvette maintained at 37°C under continuous stirring in a Horiba Jobin Yvon spectrofluorimeter. Every 22 s the cell sample was excited at 340 nm and emission was collected at 450 nm. After stabilization of the fluorescence signal, QC at the indicated dose was added directly to the cuvette, and the kinetic recording was carried on for an additional 45–60 min. The resting value of NAD(P)H fluorescence was obtained as the average intensity recorded over the final 10 min. before the addition of QC. To express the relative variation in the cellular NAD(P)H level, NAD(P)H fluorescence was normalized to the resting value. The background fluorescence obtained in a cuvette containing equivalent amounts of SS or SS and DMSO was correspondingly subtracted from all data.

2.7. Statistics. Unless indicated otherwise, the data are presented as median ± s.e.m. of at least three different measurements. Statistically significant differences were determined using Student's t-test. A level of $P < 0.05$ was considered significant in all statistical tests.

3. Results

3.1. Effects of Proton Radiation, MD, H_2O_2, QC, and EGCG on Apoptosis and Cell Cycle. First we assessed apoptosis and cell cycle distributions of Jurkat cells undergoing various treatments. The results are collected in Figure 1.

Some of our preliminary determinations indicated that high doses (10 Gy) of accelerated protons induce necrosis, not apoptosis in Jurkat cells [27]. Consistent with this, in the present study we found that irradiation with 2 Gy but not

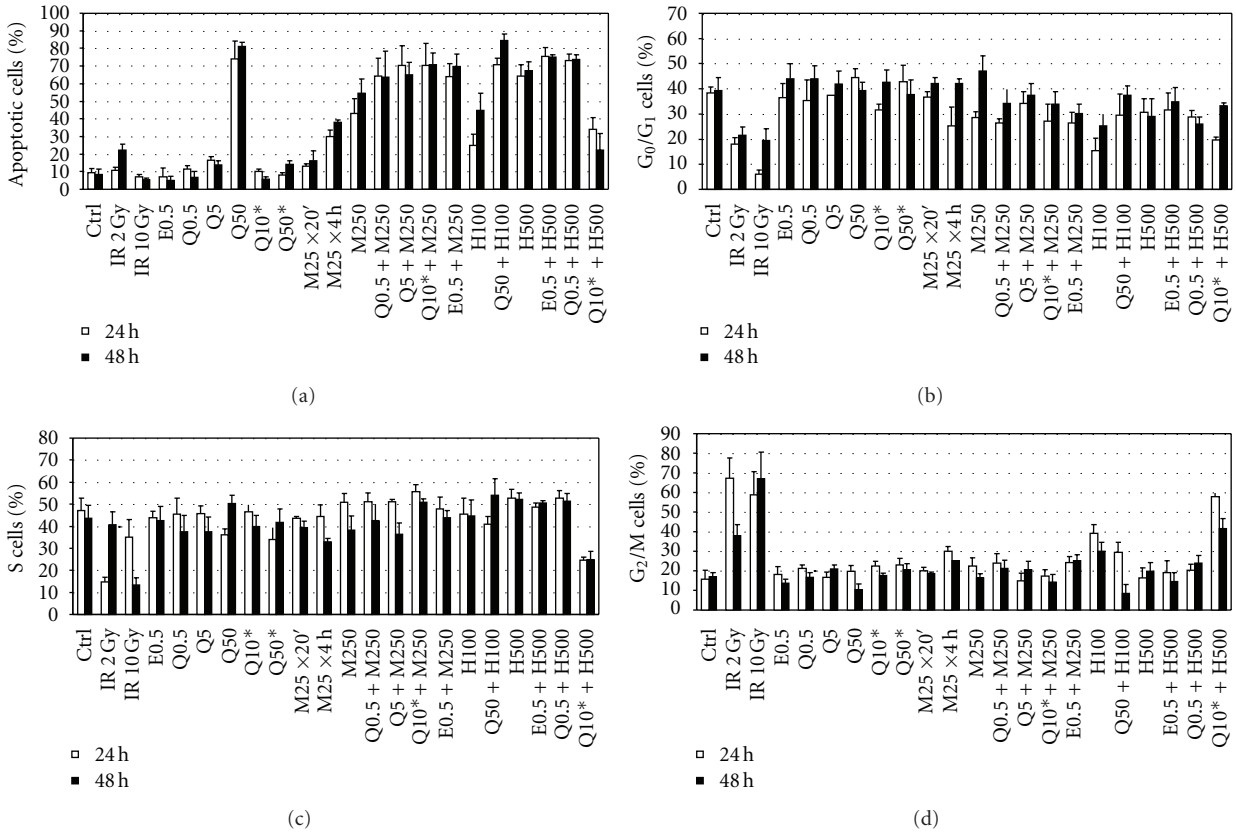

Figure 1: Apoptosis and cell-cycle distributions assessed at 24 and 48 h after treatment of Jurkat cells with the vehicle (Ctrl), with 0.5, 5 or 50 μM QC for 24 h (Q0.5, Q5, Q50), 10 or 50 μM QC for 1 h (Q10*, Q50*), 0.5 μM EGCG for 24 h (E0.5), 250 μM MD for 20 min. (M250), 100, or 500 μM H_2O_2 for 20 min. (H100 or H500) or after combined treatments (QC or EGCG preincubation followed by addition of 250 μM MD or 100/500 μM H_2O_2 for 20 min.) and after irradiation with 2 Gy or 10 Gy of protons (IR 2 Gy, IR 10 Gy). Apoptotic rates (a), G_0/G_1 (b), S-phase (c), and G_2/M (d) cell fractions are indicated.

10 Gy of high-energy protons produced a significant increase in the apoptotic rate at 48 h after irradiation (Figure 1(a), see Figure S1A,B in Supplementary Material available online at doi:10.1155/2012/498914). However, both doses consistently blocked the cell cycle at the G_2/M phase within 24 h after irradiation, suggesting the presence of severe DNA damage in irradiated cells (Figure 1(d)). There was a consistent decline in the G_2/M cell fraction at 48 h after irradiation with 2 Gy but not 10 Gy (Figure 1(d)), which was associated with a reduction in the S-cell pool (Figure 1(c)), suggesting that a part of the cells receiving 2 Gy of protons were able to initiate apoptosis from the G_2/M phase arrest whereas those receiving 10 Gy were too damaged to trigger apoptosis and to repair the DNA lesions. Indeed, clonogenic survival after irradiation with 10 Gy of protons was below the resolution of our assay (i.e., <0.1%), indicating that this dose of protons induced massive necrosis in this cell system, similar to other reports for X- or γ-irradiation [25, 29, 30]. Trypan blue exclusion tests confirmed high rates of cell death, namely, 18.4 ± 3.2% and 46.6 ± 6.8% at 24 h and 48 h after irradiation with 10 Gy of protons, respectively.

0.5 μM EGCG applied for 24 h did not affect the apoptotic rate or the cell cycle distribution (Figure 1) but could enhance apoptosis induced by MD or H_2O_2 (discussed below).

In agreement with our previous investigations [15, 27], quercetin induced apoptosis in Jurkat cells in a dose- and time-dependent manner (Figure 1(a), Figure S1C). Thus, 50 μM QC delivered for 1 h or 24 h produced at 48 h after the treatment an apoptotic rate of 14.1 ± 2.1% (Figure S1C) or 81.5 ± 2.5%, respectively, as compared with the corresponding rate of 8.4 ± 3.2% in control cells (Figure S1A). From kinetic measurements it appeared that quercetin can arrest Jurkat cells in the G_2/M phase (Figure 2). Moreover, the G_2/M fraction of cells treated with 50 μM QC for 24 h decreased from 39.8 ± 6.4% at 9 h to 10.3 ± 3.0% at 48 h after the treatment (Figure 2(d)). The G_2/M block was associated with a significant reduction in the G_0/G_1 cell fraction (Figure 2(b)), whereas the S-phase distribution was unaltered (Figure 2(c)). The cells also displayed a consistent apoptotic rate (52.2 ± 7.3%) 9 h after drug removal, which then increased gradually up to 81.5% during the probing interval (Figure 2(a)). This value is in agreement with the clonogenic survival of these cells, which was determined to be 35.9 ± 10.4% ($n = 4$). In addition, the consistent depletion of the G_2/M cell pool in the absence of significant changes in the G_0/G_1 and S-phase distributions at 48 h after the treatment suggests that a part of the G_2/M-arrested cells most likely initiated apoptosis after 1 day from the removal of quercetin.

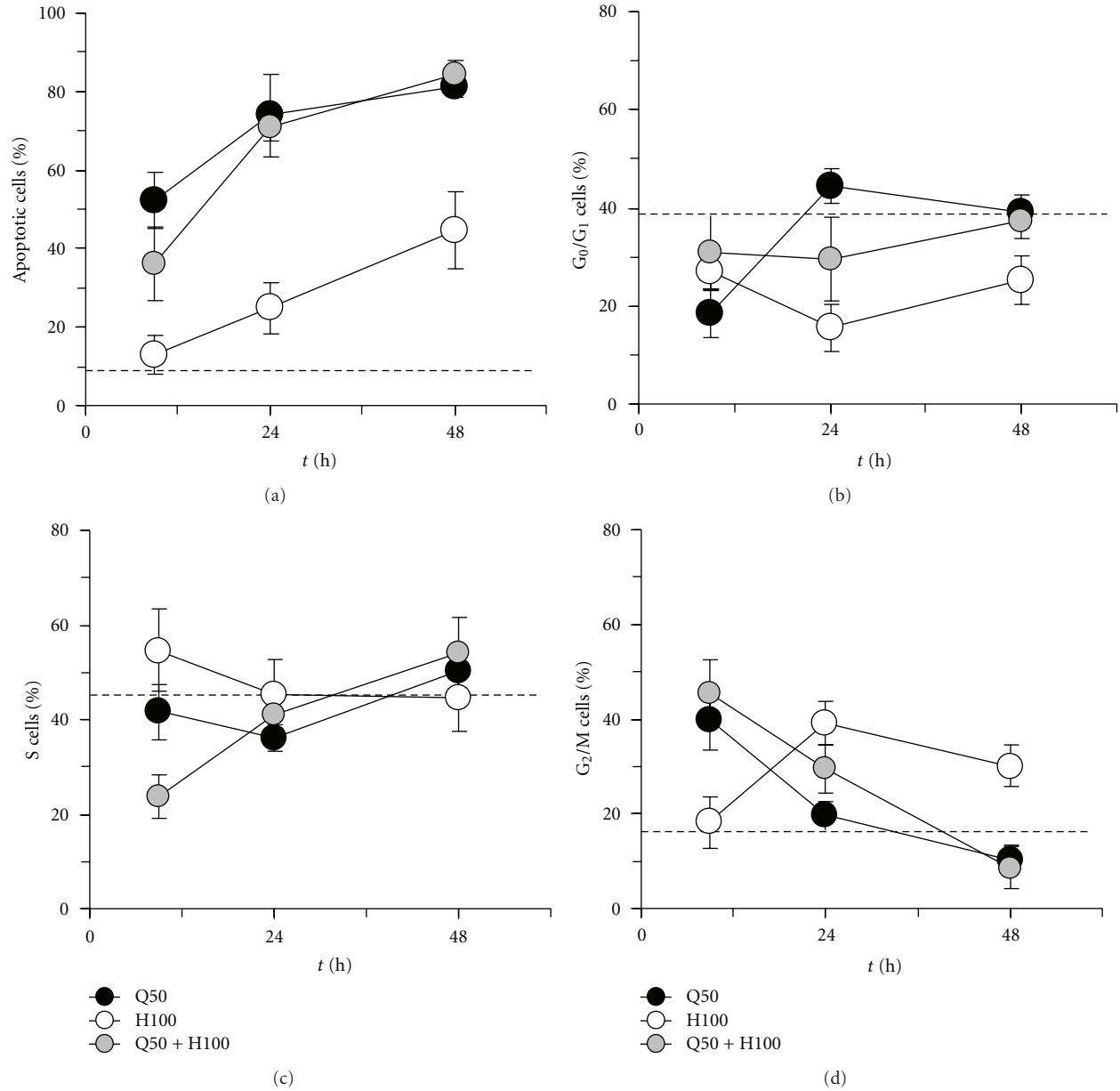

Figure 2: Time course of the apoptotic rate and cell-cycle distribution after treatment of Jurkat cells with 50 μM QC for 24 h (Q50, solid circles), 100 μM H_2O_2 for 20 min. (H100, open circles), or combination of the two (50 μM QC preincubation followed by addition of 100 μM H_2O_2 for 20 min.; treatment denoted as Q50 + H100, gray circles). Apoptotic rates (a), G_0/G_1 (b), S phase (c), and G_2/M (d) cell fractions are indicated. The dashed line represents the average obtained from control cell samples.

Menadione also induced apoptosis dose and time dependently (Figure 1(a), Figure S1D). A relatively low dose of 25 μM MD produced a consistent apoptotic rate when delivered for a long time (4 h, treatment "M25 × 4 h") but not for a short interval (20 min., treatment "M25"). The highest dose used here, 250 μM MD delivered for 20 min. (treatment "M250"), produced large apoptotic cell fractions at 24 and 48 h after the treatment (Figure S1D) and decreased clonogenic survival of Jurkat cells to 12.3 ± 3.6% ($n = 4$). A significant enhancement of apoptosis induced by 250 μM MD was obtained by preincubating Jurkat cells with 5 μM QC or 0.5 μM EGCG for 24 h, as well as with 10 μM QC for 1 h but not with 0.5 μM QC for 24 h. In general, MD, alone or in combination with QC or EGCG, decreased the G_0/G_1 cell fraction and elevated to some extent the S cell fraction in the first 24 h after the treatment (Figures 1(b) and 1(c)). The G_2/M cell fraction increased significantly in the treatments M25 × 4 h and M250, as well as in combination with a long preincubation (24 h) with very low doses of 0.5 μM QC or EGCG (Figure 1(d)). 250 μM MD applied alone for 20 min. increased significantly the G_2/M cell fraction from the control baseline of 15.7 ± 4.5% to 22.5 ± 4.3% in the first 24 h after the treatment (Figure 1(d)). The parallel decrease in the G_0/G_1 cell fraction (Figure 1(b)) and conservation of the S-phase distribution (Figure 1(c)) suggest that MD did not affect G_0/G_1 and S-phase

progression. However, during the subsequent 24 h the G_2/M block was removed and the cell cycle distribution became similar to that of control cells. At variance with this result, a persistent G_2/M arrest could be observed in cells treated with the low dose of 25 μM MD for 4 h. Furthermore, the cell cycle dynamics following this treatment suggest also a G_0/G_1 arrest that could lead to an apparently normal G_0/G_1 cell fraction and to a decline in the S-cell fraction at 48 h after the treatment. Similarly, in the EGCG-MD combination the G_2/M blockage persisted even after 48 h following the treatment, when the G_2/M cell fraction increased to 25.2 ± 2.9%. However, in this case the reduction of the G_0/G_1 cell pool and the conservation of the S-cell fraction indicate that the G_0/G_1 and S phases were not affected by this treatment.

Hydrogen peroxide acted as a potent inducer of apoptosis in Jurkat cells (Figures 1 and 2, Figure S1E). Interestingly, 100 μM H_2O_2 but not 500 μM H_2O_2 applied for 20 min. could increase significantly the G_2/M cell fraction (Figure 1(d)), suggesting that the highest dose produced severe cell damage that inhibited the activation and/or the maintenance of the G_2/M checkpoint. This conclusion was further supported by results obtained with cells exposed to 500 μM H_2O_2 after a 1 h preincubation with 10 μM QC. These cells presented a greatly reduced apoptotic rate and a considerable blockage in the G_2/M phase, as compared with the cells exposed to 500 μM H_2O_2 in the absence of QC, indicating that QC exerted an antioxidant effect and protected cells against H_2O_2. Application of 100 μM H_2O_2 for 20 min. after preincubation with 50 μM QC for 24 h induced apoptosis in a manner that was closely similar to that produced by the quercetin treatment alone (Figure 2(a)). This effect was also observed for the G_2/M cell fraction (Figure 2(d)). However, a significant difference was visible in the G_0/G_1 and S cell pools 9 h after the treatment (Figures 2(b) and 2(c)), when the S-cell fraction exhibited a marked reduction, while the G_0/G_1 fraction did not change significantly. Together, these findings suggest that, beside the observed G_2/M arrest, the combination of QC and H_2O_2 produced an additional blockage of the cell cycle in the G_0/G_1 phase as well, whereas the S phase progressed normally. However, after 48 h the cell cycle distribution became similar to that produced by quercetin alone. A significant enhancement of apoptosis induced by H_2O_2 was obtained by preincubation with 0.5 μM EGCG for 24 h (Figure 1), whereas a short incubation with 10 μM QC for 1 h exerted protective effects against H_2O_2, consistent with earlier findings [15, 27]. Thus, the apoptotic cell fraction produced by 500 μM H_2O_2 decreased 3 times, and this process was correlated with a consistent G_2/M block (Figure 1), indicating that the short preincubation with quercetin can protect cells against the deleterious effects of H_2O_2 and improve the cell capacity of repair.

In treatments with duration of 1 h, QC decreased clonogenic survival in an exponential manner, with an estimated dose for reduction of clonogenicity to 50%, $D_{50\%}$ = 109.8 μM (Figure 3(a)). In separate spectrofluorimetry experiments, QC also decreased the cellular content of NAD(P)H in a dose-dependent manner, with an effective dose for half-maximal effect IC_{50} = 39.5 μM (Figure 3(b)). In Figure 3(c) we present some examples of NAD(P)H fluorescence recordings in Jurkat cell suspensions exposed to different concentrations of QC. After addition of QC, the NAD(P)H fluorescence signal decreased slowly (in up to ~15 min.) to a steady value which appeared to be dose dependent. Figure 3(b) summarizes the steady state data obtained from recordings like those in Figure 3(c).

In a different set of experiments, we investigated the effects of preincubating Jurkat cells with 50 μM QC for 1 h on apoptosis and cell cycle distribution after irradiation with 2 Gy of protons (Figure 4, Figure S1F). Quercetin exercised an inhibitory effect on apoptosis (Figure 4(a), Figure S1F) and appeared to prolong significantly the G_2/M arrest induced by proton irradiation (Figure 4(d)), which may indicate an enhanced capacity for DNA repair and maintenance of the G_2/M checkpoint active. The parallel reduction in the S-cell pool (Figure 4(c)) and conservation of the G_0/G_1 cell fraction (Figure 4(b)) suggests that cells surviving irradiation may experience an additional G_0/G_1 but not S-phase arrest after 48 h from irradiation.

3.2. Effects of Proton Radiation, MD, H_2O_2, QC, and EGCG on Delayed Luminescence. Delayed luminescence of control cells presented a multiscale kinetics (Figure 5(a)) which could be fitted very well by a linear combination of seven exponential components (not shown). In addition to collecting all photons emitted in the entire visible domain, DL could be also measured at emission wavelengths of 460 nm and 645 nm, respectively, by using selective filters. Photoemission at these two wavelengths exhibited kinetic profiles that were qualitatively similar to that obtained in the visible domain. The intensity of emitted red light was consistently higher than the intensity of emitted blue light in the time domain 10–100 μs and was closely similar to that of blue light in the time domain 100 μs–100 ms.

DL of Jurkat cells irradiated with 10 Gy of high-energy protons exhibited different characteristics when probed at 1 h or 24 h after irradiation. Hence, a reduction of 34.1 ± 9.6% in the DL-III relative quantum yield in VIS was observed after 1 h from irradiation, whereas the cell samples probed at 24 h after irradiation exhibited an increase of 27.3 ± 8.5% in the DL-II relative quantum yield and an increase of 41.8 ± 14.3% in the time domain 10–100 ms, while all the other components of the DL emission in VIS were not significantly different from the resting DL emission (Figure 5(b)). Shortly after irradiation, DL emitted at 460 nm was similar to that of control cells; however, the surviving cells exhibited 24 h later a significant overall DL enhancement with about 35% of the control intensity (Figure 5(c)). A remarkable augmentation, up to ~1.7-fold, of blue light emission was detected for a DL component with an established time constant of 178 μs (value derived from fitting analysis, not shown; however, the distinctive peak centered on ~180 μs is clearly visible in Figure 5(c)). 1 h after irradiation, delayed emission of red light presented a significant reduction of the DL-III component, with 38.3 ± 11.5%, whereas 24 h later DL-I decreased to 76.1 ± 13.8% of control emission, and there was a significant increase of a DL component with an estimated time constant of 379 μs (Figure 5(d), and data analysis not shown).

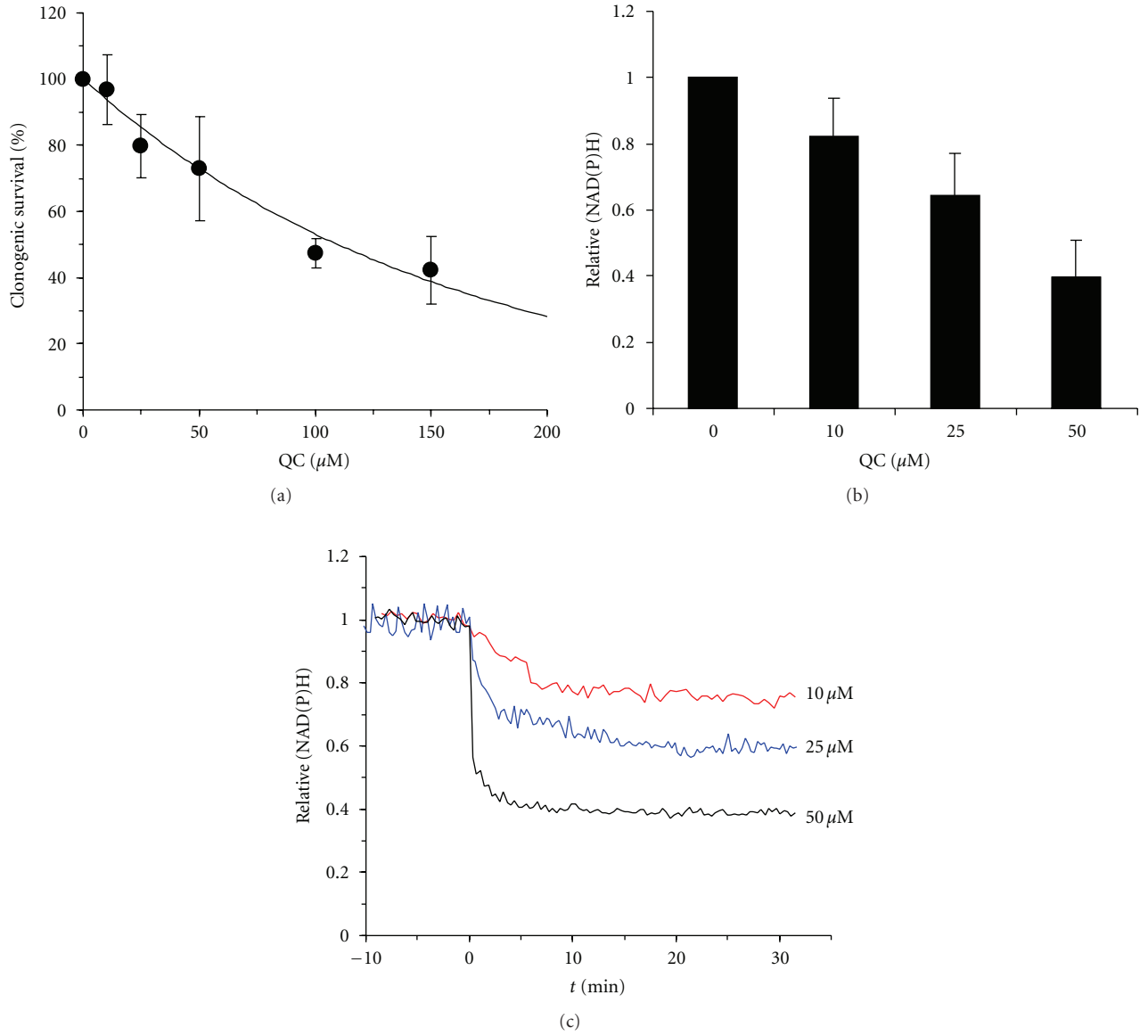

Figure 3: Quercetin decreases clonogenic survival and the cellular content of NAD(P)H in Jurkat cells. (a) Dose response of clonogenicity (S) was fitted to an exponential function (curve) of the form $S(\%) = 100 \times \exp(-D/D_0)$, where D represents the dose of QC applied for 1 h and the characteristic dose derived from the fit was $D_0 = 158.5\,\mu$M. Data are expressed as mean ± standard deviation of 4–6 separate determinations. (b) The ratio between NAD(P)H fluorescence of treated versus control cells (relative NAD(P)H) obtained in steady state after addition of QC to cell suspensions decreases with the level of QC. (c) Representative recordings of NAD(P)H fluorescence relative to the resting value in cell suspensions before and after addition of QC at various levels indicated near each trace.

At increasing doses, quercetin inhibited DL progressively (Figure 6(a)). The most sensitive DL region was DL-III, which decreased by one order of magnitude after the treatment with 50 μM QC for 24 h, whereas DL-I was only slightly affected by QC. EGCG exerted a qualitatively different effect on DL by producing a fairly uniform reduction of the photoemission intensity along the entire timescale.

500 μM H_2O_2 applied for 20 min. reduced DL significantly over the regions DL-I and DL-II (Figures 6(b), 7(a) and 7(b)). Pretreatment with 0.5 μM EGCG for 24 h was able to induce a significant recovery of DL-II emission, whereas preincubation with 10 μM QC for 1 h further reduced the DL-III intensity. The lower dose of 100 μM H_2O_2 had a modest effect on DL and inhibited photoemission by ≈22% over the entire timescale (Figures 7(a)–7(c)). Preincubation with 50 μM QC for 24 h restored DL-I emission but inhibited substantially DL-II and DL-III.

Menadione also inhibited DL in a dose-dependent manner. In addition, at variance with the modest effect of QC on DL-I, MD reduced substantially photoemission in the DL-I region (Figure 7(a)). This inhibition was strong even at the lowest dose of 25 μM menadione. DL-II was inhibited to a similar extent by high doses of MD (Figure 7(b)), whereas DL-III exhibited a drastic reduction and thus, in the M250 treatment, the DL-III quantum yield reached 15.5 ± 6.1% of its resting value (Figure 7(c)). Preincubation with the two

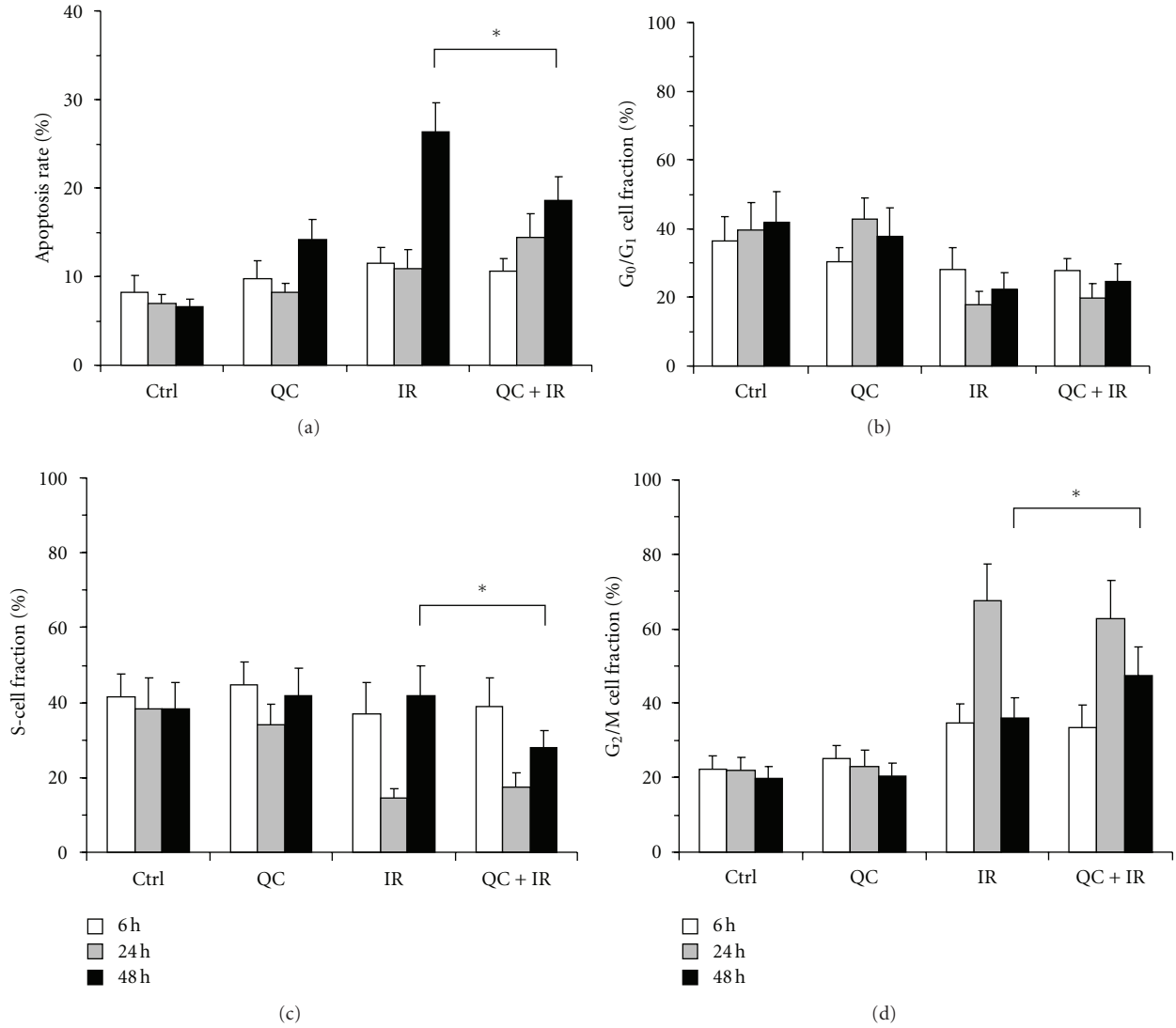

Figure 4: Apoptosis and cell-cycle distributions assessed at 6, 24, and 48 h after treatment of Jurkat cells with the vehicle (Ctrl), with 50 μM QC for 1 h (QC), with 2 Gy of proton radiation (IR), or with 2 Gy of proton radiation after preincubation with 50 μM QC for 1 h (QC + IR). Apoptotic rates (a), G_0/G_1 (b), S-phase (c), and G_2/M (d) cell fractions are illustrated. The star denotes significant difference between the treatments: IR and QC + IR.

flavonoids generally induced partial recovery of DL-III up to ~25% of the resting value, except in the case of pretreatment with 5 μM QC for 24 h, when a further reduction to 9.2 ± 3.8% was recorded.

With treatments of varying time and dosage of two oxidative stress inducers, MD and H_2O_2, and two flavonoids, QC and EGCG, as well as irradiation with high-energy protons, we obtained a significant anticorrelation ($r_{\text{all}} = -0.61$) between apoptosis and DL-II (Figure 7(e)). Notably, all MD treatments (with MD applied alone or in combination with QC or EGCG) alongside the radiation treatment were associated with a strong anticorrelation between DL-I, DL-II or DL-III, and apoptosis ($r_{\text{M/MQ/ME/IR}} = -0.76$, -0.98 and -0.84, resp.) (Figures 7(d)–7(f)). Furthermore, by selecting only treatments with MD, QC, and combinations of the two, we obtained a very strong anticorrelation between DL-II, or DL-III and apoptosis ($r_{\text{M/Q/MQ}} = -0.91$ and -0.82, resp.).

4. Discussion

At the moment, the effects of QC or EGCG on apoptosis induced in Jurkat T cells by the flavonoids themselves or in conjunction with menadione and hydrogen peroxide are poorly known. It is widely recognized that after intake, flavonoids like QC and EGCG exhibit an overall poor bioavailability, as they are rapidly metabolized and their levels in the plasma remain below 10 μM [8, 45]. However, the content of active flavonoids can increase considerably in human tissues, in particular at the inflammatory sites. In vitro studies have shown that in human normal lymphocytes, high levels of 50 μM QC can increase considerably the cellular content of $O_2^{-\bullet}$ and $OH^{\bullet}$ within 30 min. of treatment [9]. Here we found that a 24-hour treatment with physiological levels (0.5–5 μM) of QC and EGCG can potentiate the antiproliferative activity of menadione by enhancing

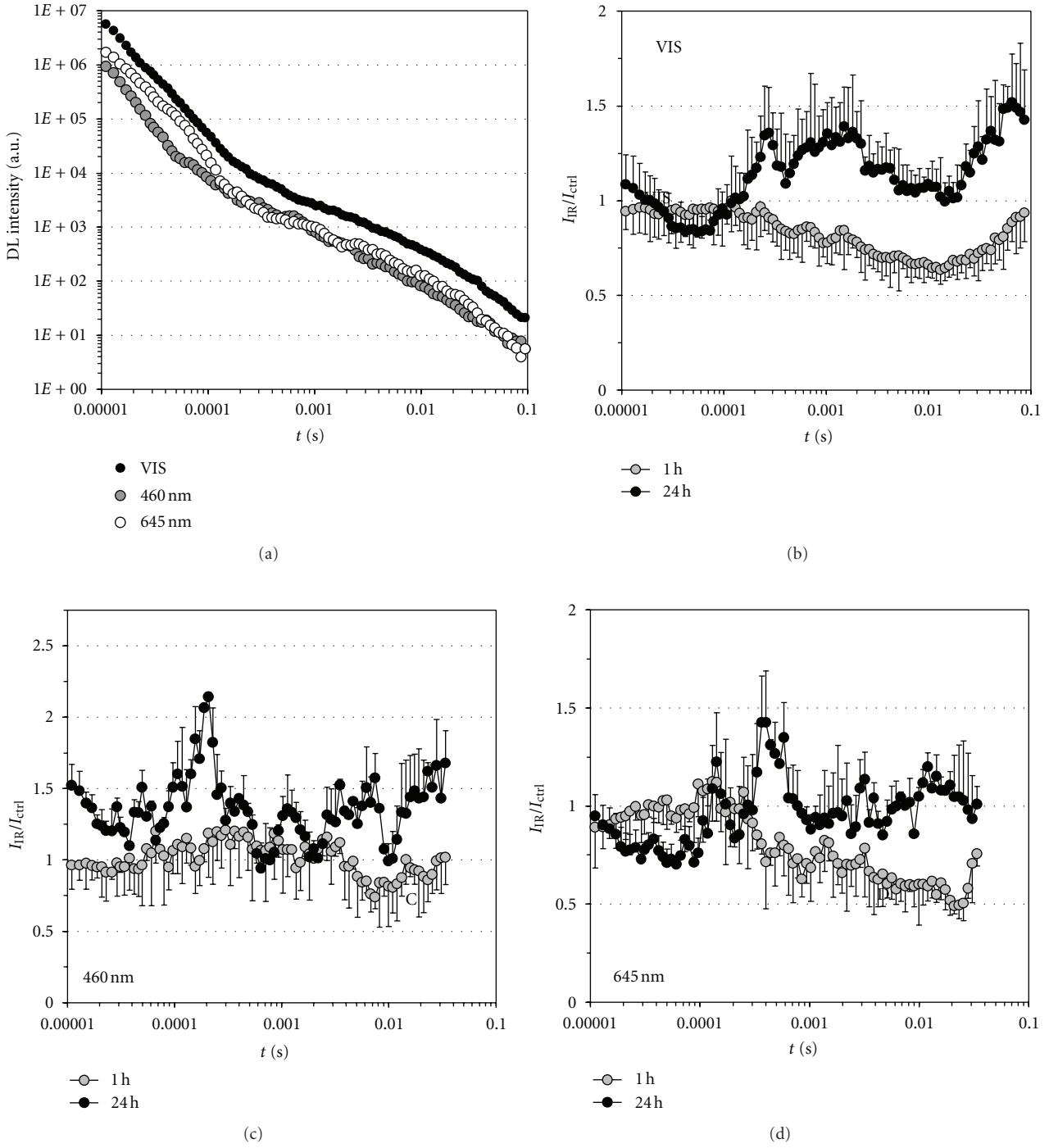

FIGURE 5: Kinetics of DL emission of Jurkat cells under control conditions (a) or after irradiation with 10 Gy of protons (b–d). In (a) some representative photoemission curves are shown for the entire visible domain (VIS), as well as for detection of 460 nm and 645 nm light emitted by the same cell sample. In (b–d) the intensity of light emission of irradiated cells (I_{IR}) is normalized to the DL intensity of sham-irradiated cultures (I_{Ctrl}). Measurements were done after 1 h and 24 h from irradiation, as indicated. Results are presented for VIS (b), 460 nm (c), and 645 nm (d) emitted light.

drug-induced apoptosis in human leukemia Jurkat T cells. In agreement with previous reports that QC is a more potent inhibitor of hydroxyl radical formation than a scavenger of superoxide anions [46], none of the quercetin-based treatments used in the present work exercised protective effects against MD, whereas a short incubation with 10 μM QC for 1 h offered consistent protection against H_2O_2 and induced G_2/M cell cycle arrest, hence allowing time for repair of H_2O_2-induced damage. In addition, preincubation for 24 h with a very low level (0.5 μM) of EGCG increased significantly the G_2/M cell fraction after exposure to 250 μM MD. Nevertheless, albeit long-term administration of QC

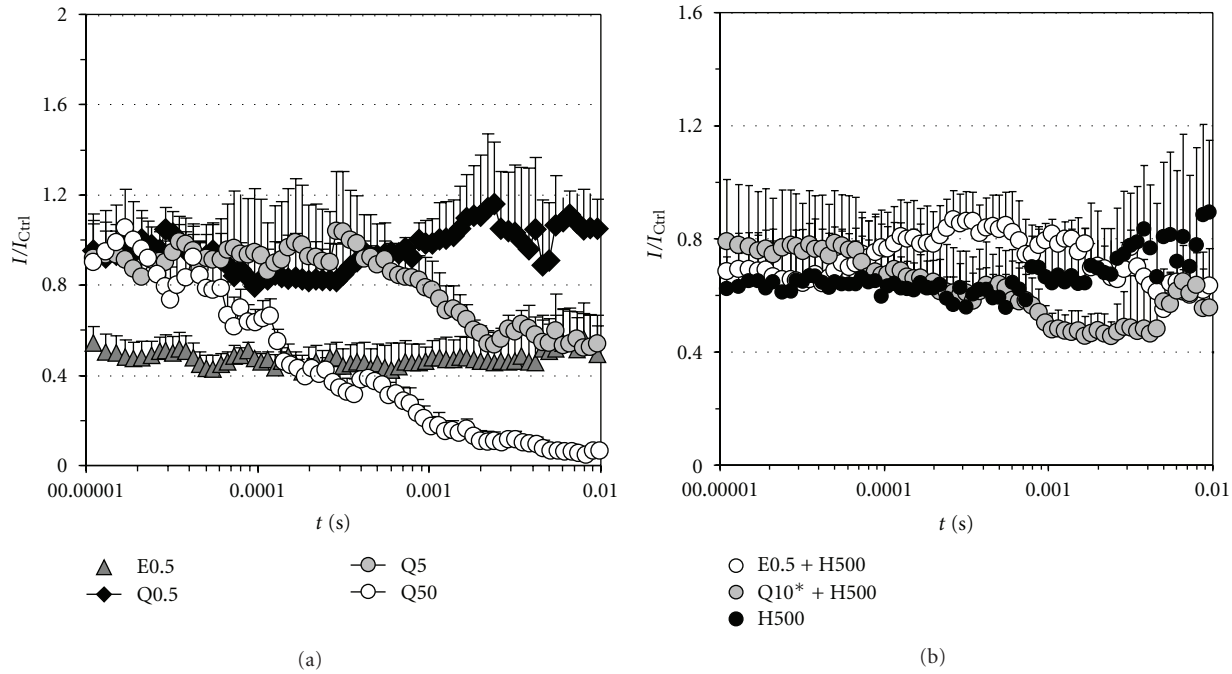

Figure 6: Kinetics of DL emission of Jurkat cells after various treatments with flavonoids (a) or with H_2O_2 alone or in combination with EGCG or QC (b). Treatments are labeled as in Figure 1. The intensity of light emission of treated cells (I) is normalized to the DL intensity of control cells (I_{Ctrl}).

or EGCG may improve significantly the menadione-based treatment of leukemia, it is important to establish the critical level of flavonoid that is no longer beneficial to normal cells.

To our knowledge, there are only few reports (e.g., [47]) regarding the effects of quercetin on clonogenic survival, which may be a critical indicator for the antiproliferative efficiency of anti-cancer drugs as well as for the likelihood of relapse after chemotherapy. While short-term treatments (1 h here) with up to 50 μM QC appeared to be effective in protecting Jurkat cells against H_2O_2 or proton irradiation, clonogenicity decreased considerably at higher doses of the flavonoid, with an estimated dose $D_{50\%}$ = 109.8 μM. Our investigations suggest a connection between the ability of quercetin to decrease the level of NAD(P)H and the induction of apoptosis, which is probably mediated by the failure to maintain the ATP-dependent electrochemical gradient across the inner mitochondrial membrane and the consequent dissipation of the mitochondrial membrane potential. The mechanism by which QC decreases the cellular content of NAD(P)H is unclear, since some early studies reported that QC can inhibit mitochondrial respiration [12], so we expected to observe an increase rather than a decrease in the NAD(P)H level. However, recent investigations based on different assays have indicated that QC can bind with high affinity to Complex I without inhibiting it [48] and can also stimulate mitochondrial respiration [10, 11]. So, it is likely that under our experimental conditions, QC actually stimulated the activity of Complex I in Jurkat cells and thus led to an increased rate of NADH consumption as a substrate for Complex I.

Interestingly, we found that 100 μM H_2O_2 but not 500 μM H_2O_2 applied for 20 min. could increase significantly the G_2/M cell fraction, suggesting that the higher dose of the oxidant agent produced more severe cell damage that inhibited the activation and/or the maintenance of the G_2/M checkpoint. A similar interesting outcome of our studies regarding the cellular effects of high-energy protons is that a higher dose (10 Gy here) of radiation could produce more damage to the apoptotic apparatus and could also reduce the capacity for DNA repair as compared with a lower dose (2 Gy here). At variance with this interpretation, an increase of ~12% in the apoptotic rate at 24 h after irradiation with 10 Gy of gamma rays was reported [29]. Moreover, it has been found that high doses (≥10 Gy) of X or γ radiation can induce significant apoptosis in Jurkat cells, in a time- and dose-dependent manner [25, 29, 30], which is in marked contrast with our findings. We then addressed this issue in a different cell type. Remarkably, in a B-lymphocyte cell line irradiated with 2 and 5 Gy of protons, respectively, the apoptotic rate and the cell-cycle distribution obtained after irradiation of these cells were qualitatively similar to those observed with Jurkat cells (not shown). Taken together, all these findings support the notion that, in comparison with the X or γ radiation, larger doses of high-energy protons produce more clusters of ionizations, which lead to more severe damage to the apoptotic or the cell cycle machinery.

Similarly to the protective effect of QC against H_2O_2 discussed above, our results suggest that short treatments with quercetin could be able to improve cell survival after proton irradiation, most likely by inhibiting hydroxyl radical formation after irradiation and protecting against cellular oxidative DNA damage. However, the fact that high-energy protons produce cellular lesions predominantly via direct ionizations, not ROS formation, together with our findings

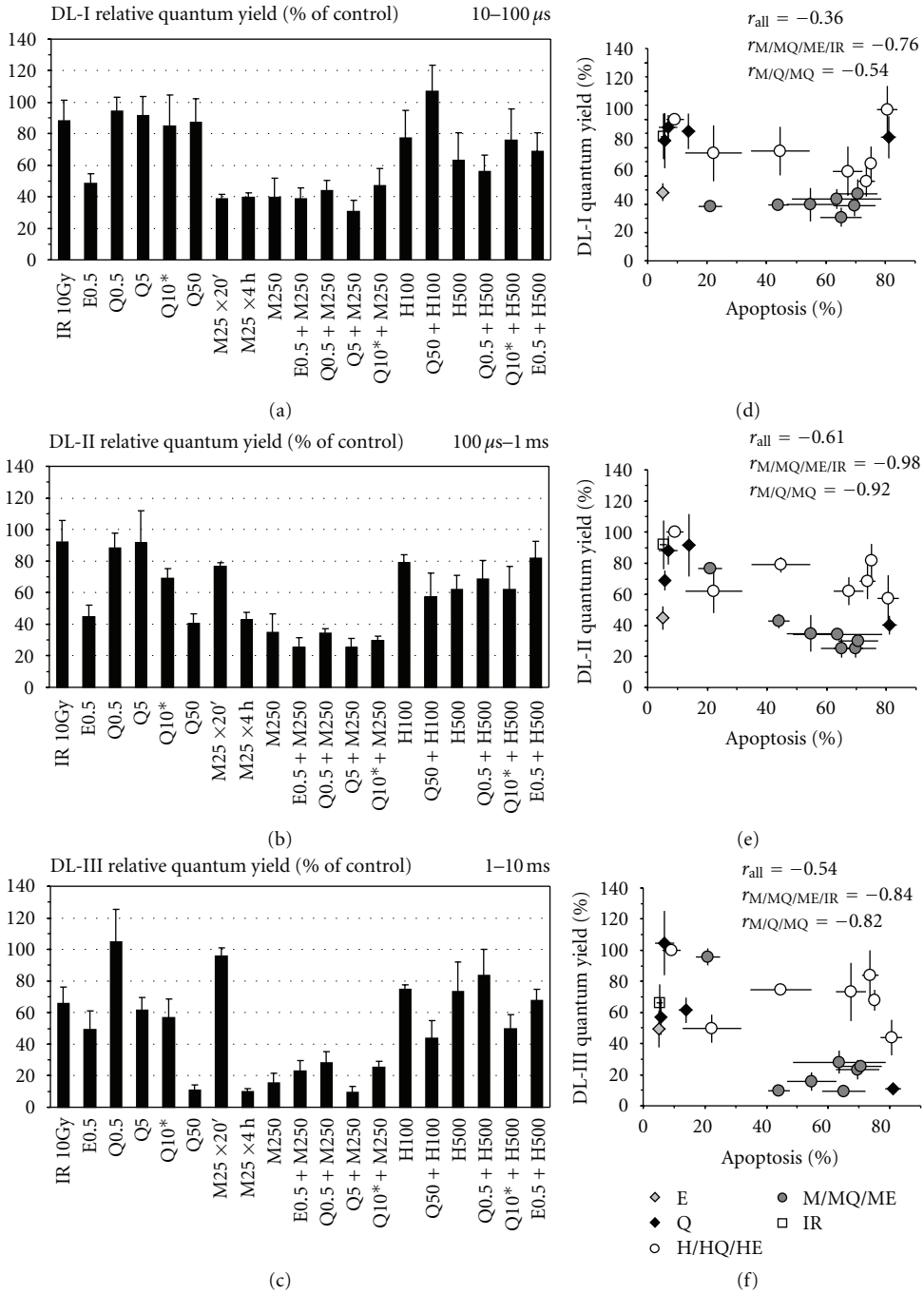

Figure 7: DL-quantum yield relative to control (a–c) and its correlation to the apoptotic cell fraction (d–f) under various treatments indicated in Figure 1. Q, E, M/MQ/ME, H/HQ/HE, and IR denote single QC or EGCG treatments, MD treatments with or without QC or EGCG preincubation, H_2O_2-treatments with or without QC or EGCG preincubation, and irradiation with 10 Gy of protons, respectively. Pearson correlation coefficients are shown for all treatments (r_{all}), for the M/MQ/ME/IR treatments ($r_{M/MQ/ME/IR}$) and for the M/Q/MQ treatments ($r_{M/Q/MQ}$). Results obtained for separate DL time domains indicated inside boxes are displayed individually for DL-I (a, d), DL-II (b, e), and DL-III (c, f).

that the protective effects of quercetin against proton-irradiation were relatively modest, suggests that quercetin may not be able to protect against the formation of the more severe lesions induced by clustered ionizations.

Our studies offer novel insights into the relationship between the cell status and delayed luminescence. In biological systems, DL may be generated by direct emitters like flavins, carbonyl derivatives, and aromatic compounds, by molecular oxygen and its various species, by the DNA or the cytoskeleton, as well as by collective molecular interactions, for example, triplet-triplet annihilation, electric field effects in membranes [31–40]. Previous data from our laboratories have indicated an important role of the mitochondrial Complex I in DL [15], consistent with earlier findings that

some electron transport inhibitors can reduce light emission by mitochondria and chloroplasts [41–43]. In Complex I, the two electrons delivered by reduced nicotinamide adenine dinucleotide (NADH) to flavine mononucleotide (FMN) are transferred between eight consecutive iron-sulfur clusters, eventually reaching the ubiquinone. Our earlier findings [15] suggested that upon UV irradiation, FMN can produce excited singlet states that may either decay to the ground state by prompt fluorescence [49] or undergo intersystem crossing to long-lived triplet states [50] which can subsequently relax to some metastable intermediate states [50]. These triplet- or metastable-state species exhibit an intrinsically long lifetime, allowing a series of photochemical reactions to occur in Complex I via charge recombination in the Fe/S redox centers and then produce secondary excitations, hence giving rise to delayed luminescence.

The data presented here indicate that DL of proton-irradiated cells probed shortly after irradiation was dominated by light emission in the red region of the spectrum and was characterized by a significant reduction in the millisecond DL-III region. On the contrary, DL emission of irradiated cells that survived the subsequent 24 h was dominated by light emission in the blue region of the spectrum and exhibited a significant increase in the submillisecond DL-II region. Moreover, cells that survived 1 day postirradiation revealed two distinctive DL states, namely, a blue-light emitting state with a characteristic lifetime of 178 μs and a red-light emitting state with a characteristic lifetime of 379 μs. In agreement with our previous results [15] and a series of data we have obtained with rotenone-treated cells (not shown), as well as with established electron transfer rates within Complex I [51], we propose that the red-light emitting state is characteristic to the Fe/S center N2 in reduced form. Given the value of the characteristic lifetime of the blue-light emitting state, it is likely that this state is connected to the other extreme Fe/S center, namely, N1a, which has a similar time constant for its reduction rate [51]. In addition, the DL-III region may reflect the reduction kinetics of the remaining redox centers of Complex I that reside between the two extreme N1a and N2 centers, which have been determined to exhibit a slow reduction on the millisecond scale [51]. Accordingly, our data suggest that immediately after irradiation there is a significant decline in the pool of reduced intermediary Fe/S centers, whereas after 24 h there is a significant increase in the pool of reduced N1a and N2 centers. It means that on short-term high-energy protons can disrupt the electron transfer within Complex I, either by lowering the cellular content of NADH (directly and/or indirectly) and thus decreasing the availability of NADH for binding to Complex I or by directly altering the structure or the functionality of Complex I. However, surviving cells appear to regain functionality of Complex I within one day from irradiation, yet manifesting a partial inhibition at the level of the centers N1a and N2.

We found previously that QC and MD at high doses exhibited virtually identical effects on DL over a wide time interval, from 100 μs to 10 ms after laser excitation [15], probably due to their similar action at the level of Complex I. After measuring superoxide production at Complex I by menadione, Xu and Arriaga concluded that Complex I may accept an electron from menadione at a specific site of Complex I [52]. Our results obtained by DL spectroscopy suggest an equivalent action of MD and QC at the level of the Fe/S center N2, which may be mediated by the binding of each of these molecules to a common site in Complex I. Having in view the structural similarity between QC and rotenone, it is most likely that the QC/MD site is the rotenone-binding site itself [48], which resides near the center N2 and thus allows the bound molecule of rotenone to hinder the electron transfer from N2 to ubiquinone.

The faster DL region, DL-I, exhibited the most variable response to our treatment conditions. QC and proton irradiation did not affect DL-I, while MD and EGCG reduced consistently DL-I even at low doses. Taking into consideration all the results presented here, we suppose that DL-I may be associated with the photoemission characteristics of FMN, not with its availability to donate electrons to the two neighbor centers, N1a and N3, whose reduction takes place on a slower timescale [51] or with its association with NADH. According to this scenario, MD, EGCG, and H_2O_2, but not QC, may directly interact with FMN and alter its electronic configuration, thus reducing DL emission.

Nevertheless, these points need to be further addressed by detailed investigations with specific inhibitors of Complex I. However, it is noteworthy that our previous studies using Jurkat cells [15] and a different cell system [38], the budding yeast *Saccharomyces cerevisiae*, have indicated that DL is correlated with the activity of the Complex I of the mitochondrial respiratory chain but not with the existence of DNA or microtubule damage. Remarkably, these two different cell types, as well as the human glioblastoma U87 cell line produced a closely similar DL emission profile under control conditions (not shown). Taken together, these findings suggest that DL may not be cell-type specific and encourage further studies toward the use of DL spectroscopy in investigating mitochondrial dysfunctions in various diseases or in cancer diagnosis. Having in view the growing interest of using DL spectroscopy in clinical applications [31–35], our results lend further support for the development of this methodology as a valuable tool of investigation and diagnosis.

Acknowledgments

This work is partially supported by the Sectorial Operational Programme Human Resources Development (SOP HRD), financed from the European Social Fund and by the Romanian Government under the Contract no. POSDRU/89/1.5/S/64109 and by a Grant of the Romanian National Authority for Scientific Research, CNCS-UEFISCDI, Project no. PN-II-ID-PCE-2011-3-0800, no. 342/2011.

References

[1] M. K. Johnson and G. Loo, "Effects of epigallocatechin gallate and quercetin on oxidative damage to cellular DNA," *Mutation Research—DNA Repair*, vol. 459, no. 3, pp. 211–218, 2000.

[2] D. W. Han, M. H. Lee, H. H. Kim, S. H. Hyon, and J. C. Park, "Epigallocatechin-3-gallate regulates cell growth, cell cycle and phosphorylated nuclear factor-κB in human dermal fibroblasts," *Acta Pharmacologica Sinica*, vol. 32, no. 5, pp. 637–646, 2011.

[3] C. Stresemann, B. Brueckner, T. Musch, H. Stopper, and F. Lyko, "Functional diversity of DNA methyltransferase inhibitors in human cancer cell lines," *Cancer Research*, vol. 66, no. 5, pp. 2794–2800, 2006.

[4] H. Wu, B. Zhu, Y. Shimoishi, Y. Murata, and Y. Nakamura, "(-)-Epigallocatechin-3-gallate induces up-regulation of Th1 and Th2 cytokine genes in Jurkat T cells," *Archives of Biochemistry and Biophysics*, vol. 483, no. 1, pp. 99–105, 2009.

[5] H. Nakagawa, K. Hasumi, J. T. Woo, K. Nagai, and M. Wachi, "Generation of hydrogen peroxide primarily contributes to the induction of Fe(II)-dependent apoptosis in Jurkat cells by (-) -epigallocatechin gallate," *Carcinogenesis*, vol. 25, no. 9, pp. 1567–1574, 2004.

[6] S. Matzno, Y. Yamaguchi, T. Akiyoshi, T. Nakabayashi, and K. Matsuyama, "An attempt to evaluate the effect of vitamin K3 using as an enhancer of anticancer agents," *Biological and Pharmaceutical Bulletin*, vol. 31, no. 6, pp. 1270–1273, 2008.

[7] D. Chen, K. G. Daniel, M. S. Chen, D. J. Kuhn, K. R. Landis-Piwowar, and Q. P. Dou, "Dietary flavonoids as proteasome inhibitors and apoptosis inducers in human leukemia cells," *Biochemical Pharmacology*, vol. 69, no. 10, pp. 1421–1432, 2005.

[8] J. H. Jeong, J. Y. An, Y. T. Kwon, J. G. Rhee, and Y. J. Lee, "Effects of low dose quercetin: cancer cell-specific inhibition of cell cycle progression," *Journal of Cellular Biochemistry*, vol. 106, no. 1, pp. 73–82, 2009.

[9] G. C. Yen, P. D. Duh, H. L. Tsai, and S. L. Huang, "Pro-oxidative properties of flavonoids in human lymphocytes," *Bioscience, Biotechnology and Biochemistry*, vol. 67, no. 6, pp. 1215–1222, 2003.

[10] M. Fiorani, A. Guidarelli, M. Blasa et al., "Mitochondria accumulate large amounts of quercetin: prevention of mitochondrial damage and release upon oxidation of the extramitochondrial fraction of the flavonoid," *Journal of Nutritional Biochemistry*, vol. 21, no. 5, pp. 397–404, 2010.

[11] U. de Marchi, L. Biasutto, S. Garbisa, A. Toninello, and M. Zoratti, "Quercetin can act either as an inhibitor or an inducer of the mitochondrial permeability transition pore: a demonstration of the ambivalent redox character of polyphenols," *Biochimica et Biophysica Acta*, vol. 1787, no. 12, pp. 1425–1432, 2009.

[12] D. J. Dorta, A. A. Pigoso, F. E. Mingatto et al., "The interaction of flavonoids with mitochondria: effects on energetic processes," *Chemico-Biological Interactions*, vol. 152, no. 2-3, pp. 67–78, 2005.

[13] D. Metodiewa, A. K. Jaiswal, N. Cenas, E. Dickancaité, and J. Segura-Aguilar, "Quercetin may act as a cytotoxic prooxidant after its metabolic activation to semiquinone and quinoidal product," *Free Radical Biology and Medicine*, vol. 26, no. 1-2, pp. 107–116, 1999.

[14] R. Ferraresi, L. Troiano, E. Roat et al., "Essential requirement of reduced glutathione (GSH) for the anti-oxidant effect of the flavonoid quercetin," *Free Radical Research*, vol. 39, no. 11, pp. 1249–1258, 2005.

[15] I. Baran, C. Ganea, A. Scordino et al., "Effects of menadione, hydrogen peroxide, and quercetin on apoptosis and delayed luminescence of human leukemia jurkat T-cells," *Cell Biochemistry and Biophysics*, vol. 58, no. 3, pp. 169–179, 2010.

[16] G. N. Kim and H. D. Jang, "Protective mechanism of quercetin and rutin using glutathione metabolism on H_2O_2-induced oxidative stress in HepG2 cells," *Annals of the New York Academy of Sciences*, vol. 1171, pp. 530–537, 2009.

[17] B. M. Kim, Y. J. Choi, Y. Han, Y. S. Yun, and S. H. Hong, "N,N-dimethyl phytosphingosine induces caspase-8-dependent cytochrome *c* release and apoptosis through ROS generation in human leukemia cells," *Toxicology and Applied Pharmacology*, vol. 239, no. 1, pp. 87–97, 2009.

[18] S. Piyaviriyakul, K. Shimizu, T. Asakawa, T. Kan, P. Siripong, and N. Oku, "Anti-angiogenic activity and intracellular distribution of epigallocatechin-3-gallate analogs," *Biological and Pharmaceutical Bulletin*, vol. 34, no. 3, pp. 396–400, 2011.

[19] I. Laux and A. Nel, "Evidence that oxidative stress-induced apoptosis by menadione involves Fas-dependent and Fas-independent pathways," *Clinical Immunology*, vol. 101, no. 3, pp. 335–344, 2001.

[20] J. J. Brière, D. Schlemmer, D. Chretien, and P. Rustin, "Quinone analogues regulate mitochondrial substrate competitive oxidation," *Biochemical and Biophysical Research Communications*, vol. 316, no. 4, pp. 1138–1142, 2004.

[21] M. Floreani and F. Carpenedo, "One- and two-electron reduction of menadione in guinea-pig and rat cardiac tissue," *General Pharmacology*, vol. 23, no. 4, pp. 757–762, 1992.

[22] A. Rasola and M. Geuna, "A flow cytometry assay simultaneously detects independent apoptotic parameters," *Cytometry*, vol. 45, pp. 151–157, 2001.

[23] W. Yin, X. Li, S. Feng et al., "Plasma membrane depolarization and Na,K-ATPase impairment induced by mitochondrial toxins augment leukemia cell apoptosis via a novel mitochondrial amplification mechanism," *Biochemical Pharmacology*, vol. 78, no. 2, pp. 191–202, 2009.

[24] S. Y. Chien, Y. C. Wu, J. G. Chung et al., "Quercetin-induced apoptosis acts through mitochondrial- and caspase-3-dependent pathways in human breast cancer MDA-MB-231 cells," *Human and Experimental Toxicology*, vol. 28, no. 8, pp. 493–503, 2009.

[25] D. E. Godar, "UVA1 radiation triggers two different final apoptotic pathways," *Journal of Investigative Dermatology*, vol. 112, no. 1, pp. 3–12, 1999.

[26] J. H. Wang, J. Cheng, C. R. Li, M. Ye, Z. Ma, and F. Cai, "Modulation of Ca^{2+} signals by epigallocatechin-3-gallate(EGCG) in cultured rat hippocampal neurons," *International Journal of Molecular Sciences*, vol. 12, no. 1, pp. 742–754, 2011.

[27] I. Baran, C. Ganea, A. Scordino et al., "Apoptosis, cell cycle and delayed luminescence of human leukemia Jurkat T-cells under proton-irradiation and oxidative stress conditions," in *Activity Report Istituto Nazionale Di Fisica Nucleare Laboratori Nazionali Del Sud*, pp. 246–249, Arti Grafiche Le Ciminiere Catania, Catania, Italia, 2010.

[28] I. Verbrugge, E. H. J. Wissink, R. W. Rooswinkel et al., "Combining radiotherapy with APO010 in cancer treatment," *Clinical Cancer Research*, vol. 15, no. 6, pp. 2031–2038, 2009.

[29] S. F. Zerp, R. Stoter, G. Kuipers et al., "AT-101, a small molecule inhibitor of anti-apoptotic Bcl-2 family members, activates the SAPK/JNK pathway and enhances radiation-induced apoptosis," *Radiation Oncology*, vol. 4, no. 1, article 47, 2009.

[30] B. Gong and A. Almasan, "Apo2 ligand/TNF-related apoptosis-inducing ligand and death receptor 5 mediate the apoptotic signaling induced by ionizing radiation in leukemic cells," *Cancer Research*, vol. 60, no. 20, pp. 5754–5760, 2000.

[31] M. A. E. J. Ortner, B. Ebert, E. Hein et al., "Time gated fluorescence spectroscopy in Barrett's oesophagus," *Gut*, vol. 52, no. 1, pp. 28–33, 2003.

[32] F. Musumeci, L. A. Applegate, G. Privitera, A. Scordino, S. Tudisco, and H. J. Niggli, "Spectral analysis of laser-induced ultraweak delayed luminescence in cultured normal and tumor human cells: temperature dependence," *Journal of Photochemistry and Photobiology B*, vol. 79, no. 2, pp. 93–99, 2005.

[33] H. W. Kim, S. B. Sim, C. K. Kim et al., "Spontaneous photon emission and delayed luminescence of two types of human lung cancer tissues: adenocarcinoma and Squamous cell carcinoma," *Cancer Letters*, vol. 229, no. 2, pp. 283–289, 2005.

[34] W. Kemmner, K. Wan, S. Rüttinger et al., "Silencing of human ferrochelatase causes abundant protoporphyrin-IX accumulation in colon cancer," *The FASEB Journal*, vol. 22, no. 2, pp. 500–509, 2008.

[35] E. G. Mik, T. Johannes, C. J. Zuurbier et al., "*In vivo* mitochondrial oxygen tension measured by a delayed fluorescence lifetime technique," *Biophysical Journal*, vol. 95, no. 8, pp. 3977–3990, 2008.

[36] V. Goltsev, P. Chernev, I. Zaharieva, P. Lambrev, and R. J. Strasser, "Kinetics of delayed chlorophyll a fluorescence registered in milliseconds time range," *Photosynthesis Research*, vol. 84, no. 1–3, pp. 209–215, 2005.

[37] Y. Guo and J. Tan, "A kinetic model structure for delayed fluorescence from plants," *BioSystems*, vol. 95, no. 2, pp. 98–103, 2009.

[38] I. Baran, C. Ganea, I. Ursu et al., "Effects of nocodazole and ionizing radiation on cell proliferation and delayed luminescence," *Romanian Journal of Physics*, vol. 54, no. 5-6, pp. 557–567, 2009.

[39] S. Tudisco, A. Scordino, G. Privitera, I. Baran, and F. Musumeci, "ARETUSA—advanced research equipment for fast ultraweak luminescence analysis: new developments," *Nuclear Instruments and Methods in Physics Research A*, vol. 518, no. 1-2, pp. 463–464, 2004.

[40] J. Slawinski, "Luminescence research and its relation to ultraweak cell radiation," *Experientia*, vol. 44, no. 7, pp. 559–571, 1988.

[41] P. Felker, S. Izawa, N. E. Good, and A. Haug, "Effects of electron transport inhibitors on millisecond delayed light emission from chloroplasts," *Biochimica et Biophysica Acta*, vol. 325, no. 1, pp. 193–196, 1973.

[42] E. Hideg, M. Kobayashi, and H. Inaba, "Spontaneous ultraweak light emission from respiring spinach leaf mitochondria," *Biochimica et Biophysica Acta*, vol. 1098, no. 1, pp. 27–31, 1991.

[43] M. Katsumata, A. Takeuchi, K. Kazumura, and T. Koike, "New feature of delayed luminescence: preillumination-induced concavity and convexity in delayed luminescence decay curve in the green alga *Pseudokirchneriella subcapitata*," *Journal of Photochemistry and Photobiology B*, vol. 90, no. 3, pp. 152–162, 2008.

[44] I. Baran, C. Ganea, I. Ursu et al., "Fluorescence properties of quercetin in human leukemia Jurkat T-Cells," *Romanian Journal of Physics*, vol. 56, no. 3-4, pp. 388–398, 2011.

[45] D. Erba, P. Riso, A. Colombo, and G. Testolin, "Supplementation of Jurkat T cells with green tea extract decreases oxidative damage due to iron treatment," *Journal of Nutrition*, vol. 129, no. 12, pp. 2130–2134, 1999.

[46] L. C. Wilms, J. C. S. Kleinjans, E. J. C. Moonen, and J. J. Briedé, "Discriminative protection against hydroxyl and superoxide anion radicals by quercetin in human leucocytes *in vitro*," *Toxicology In Vitro*, vol. 22, no. 2, pp. 301–307, 2008.

[47] C. Carrasco-Pozo, M. L. Mizgier, H. Speisky, and M. Gotteland, "Differential protective effects of quercetin, resveratrol, rutin and epigallocatechin gallate against mitochondrial dysfunction induced by indomethacin in Caco-2 cells," *Chemico-Biological Interactions*, vol. 195, pp. 199–205, 2012.

[48] T. Samuel, K. Fadlalla, L. Mosley, V. Katkoori, T. Turner, and U. Manne, "Dual-mode interaction between quercetin and DNA-damaging drugs in cancer cells," *Anticancer Research*, vol. 32, pp. 61–71, 2012.

[49] K. A. Foster, F. Galeffi, F. J. Gerich, D. A. Turner, and M. Müller, "Optical and pharmacological tools to investigate the role of mitochondria during oxidative stress and neurodegeneration," *Progress in Neurobiology*, vol. 79, no. 3, pp. 136–171, 2006.

[50] T. E. Swartz, S. B. Corchnoy, J. M. Christie et al., "The photocycle of a flavin-binding domain of the blue light photoreceptor phototropin," *Journal of Biological Chemistry*, vol. 276, no. 39, pp. 36493–36500, 2001.

[51] M. L. Verkhovskaya, N. Belevich, L. Euro, M. Wikström, and M. I. Verkhovsky, "Real-time electron transfer in respiratory complex I," *Proceedings of the National Academy of Sciences of the United States of America*, vol. 105, no. 10, pp. 3763–3767, 2008.

[52] X. Xu and E. A. Arriaga, "Qualitative determination of superoxide release at both sides of the mitochondrial inner membrane by capillary electrophoretic analysis of the oxidation products of triphenylphosphonium hydroethidine," *Free Radical Biology and Medicine*, vol. 46, no. 7, pp. 905–913, 2009.